

MAGNETIC CLASSIFICATION OF ANTARCTIC STONY METEORITES (III)

Takesi NAGATA

National Institute of Polar Research, Kaga 1-chome, Itabashi-ku, Tokyo 173

Abstract: The Prior rule in regard to a relation between $\text{Fe}^\circ + \text{Ni}^\circ$ and $\text{Fe}^\circ/\text{Ni}^\circ$ and the Urey-Craig-Mason law in regard to a relation between Fe content in FeO and Fe content in metal and FeS for chondrites are reconfirmed on 14 newly analyzed chondrites.

It is then experimentally confirmed that the saturation magnetization (I_s) can reasonably well represent $\text{Fe}^\circ + \text{Ni}^\circ$ or Fe° in stony meteorites except carbonaceous chondrites, and that thermomagnetic parameters such as the main magnetic transition temperature (θ_c^*) in the cooling process, the ratio of α -phase magnetization to the total magnetization ($I_s(\alpha)/I_s$) and Ni-content in metallic phase ($\text{Ni}^\circ/(\text{Fe}^\circ + \text{Ni}^\circ)$) derived from the magnetic analysis are well correlated with $\text{Fe}^\circ/\text{Ni}^\circ$, whereas the θ_c^* -value for carbonaceous chondrites uniquely represents Curie point of magnetite.

E-, H-, L-, LL- and C-chondrites and achondrites are expressed as mutually well separated groups on an I_s versus $I_s(\alpha)/I_s$ diagram and an I_s versus θ_c^* diagram. On an I_s versus $\text{Ni}^\circ/(\text{Fe}^\circ + \text{Ni}^\circ)$ diagram, the five chondrite groups are well separately grouped, but the achondrite group partially overlaps the C-chondrite group domain. Synthetically using the three diagrams, however, the six stony meteorite groups can be satisfactorily identified on the basis of magnetic data alone.

1. Introduction Urey-Craig Diagram and Prior Rule for Antarctic Yamato Stony Meteorites

It has been established by UREY and CRAIG (1953) and MASON (1962) that the total sum of metallic iron (Fe°), Fe in troilite (FeS) and oxidized iron in non-metallic minerals in the chondritic meteorites is approximately constant. The metallic iron and Fe in FeS is the richest and the abundance of FeO is the poorest in the enstatite chondrites (E), the content of FeO increasing while the sum of Fe° and Fe in FeS decreasing in the successive order from E through olivine-bronzite chondrites (H), olivine-hypersthene chondrites (L) and olivine-pigeonite chondrites (LL) toward carbonaceous chondrites (C), which contain no or very little amount of metallic iron. Dealing with more detail, however, the total amount of Fe in H-chondrites (about 28.6 wt%) (UREY and CRAIG, 1953) is considerably larger than that in L-chondrites (about 22.3 wt%; UREY and CRAIG, 1953). As illustrated

in Fig. 1, the five different types of chondrites, *i.e.*, E, H, L, LL and C are well separately grouped in the diagram of the content of Fe° and Fe in FeS versus the oxidized iron content compiled by MASON (1962). Accordingly, this kind of diagram for chondritic meteorites is called a Urey-Craig diagram or a Urey-Craig-Mason diagram.

Among a number of stony meteorites which have been magnetically examined by the author and his colleagues, 14 chondrites and 2 achondrites have been chemically analyzed to date. The contents of Fe° , Ni° (metal), Co° (metal), FeS and FeO in these stony meteorites are summarized in Table 1. The Urey-Craig-Mason diagram for the 14 chondrites is shown in Fig. 2, where the five different types of chondrites are well separately grouped except a strongly weathered H-chondrite (Yamato-7301 (j)), and each group within the diagram coordinates in Fig. 2 is well identified to that in Fig. 1.

On the other hand, PRIOR (1920) pointed out that the ratio of Ni° content to Fe° content ($\text{Ni}^\circ/\text{Fe}^\circ$) decreases while the metallic phase content ($\text{Fe}^\circ + \text{Ni}^\circ$) decreases with an increase of $\text{FeO}/(\text{FeO} + \text{MgO})$ in chondrites. This relationship between the metallic phase and the silicate phase composition for chondrites have been called Prior's rule. This Prior's rule indicates that there is a positive correlation between $\text{Fe}^\circ/\text{Ni}^\circ$ and $(\text{Fe}^\circ + \text{Ni}^\circ)$ for the metallic components in chondrites. Using existing chemical data of chondrites, WASILEWSKI (1975) has actually demonstrated an almost linear relationship between $\text{Fe}^\circ/\text{Ni}^\circ$ and the total metal content for H-, L- and LL-chondritic meteorite groups. In Fig. 3, ratios $\text{Fe}^\circ/\text{Ni}^\circ$ for E-, H-, L- and LL-chondrites listed in Table 1 are plotted against their $(\text{Fe}^\circ + \text{Ni}^\circ)$ contents. In this diagram also, the four different types of chondrites are well separately grouped except the strongly weathered H-chondrite, and there is an approximately linear relation between $(\text{Fe}^\circ/\text{Ni}^\circ)$ and $(\text{Fe}^\circ + \text{Ni}^\circ)$. The carbonaceous chondrites are the most oxidized chondrites, containing no or a very small amount of metallic composition, so that carbonaceous chondrites are excluded from Fig. 3. However, considerable parts of the oxidized iron in carbonaceous chondrites form magnetites or substituted magnetites which are ferrimagnetic.

Among the mineral compositions in the stony meteorites, the metallic components comprising mostly iron and nickel are ferromagnetic; magnetites and substituted magnetites are ferrimagnetic; troilites and ilmenites are antiferromagnetic, while the other silicate minerals containing FeO such as olivines and pyroxenes are paramagnetic. Consequently, an approximate value of content of metallic component in stony meteorites can be estimated by measuring the ferromagnetic component by a magnetic method.

As illustrated in Figs. 1, 2 and 3, and as given in Table 1, the metallic phase content represented mostly by $(\text{Fe}^\circ + \text{Ni}^\circ)$ and the metallic phase composition represented mainly by $\text{Fe}^\circ/\text{Ni}^\circ$ in chondritic meteorites are sensitively and separately dependent upon chondrite types, E, H, L and LL. Hence, the magnetic estimate

Table 1. Contents of metals, FeS and FeO in stony meteorites.

Meteorites	Fe ^o	Ni ^o	Co ^o (wt%)	FeS	FeO	Fe ^o /Ni ^o
(E-chondrite)						
Yamato-691 (a)	22.18	1.86	0.089	11.47	0.48	11.92
(H-chondrite)						
Yamato-694 (d)	12.45	1.52	0.081	5.32	12.32	8.19
Yamato-7301 (j)*	7.21	0.77	0.05	5.05	18.92	9.36
Kesen	18.23	1.59	0.09	5.78	9.47	11.47
(L-chondrite)						
Yamato-7305 (k)	7.64	0.96	0.06	7.57	13.10	7.96
Yamato-7304 (m)	7.50	0.83	0.06	8.44	13.02	9.04
Yamato-74191	5.66	0.85	0.03	5.01	14.68	6.66
Fukutomi	9.83	1.33	0.02	6.37	11.62	7.39
Mino	7.86	1.16	0.05	5.88	14.48	6.78
(LL-chondrite)						
Yamato-74442	2.48	0.99	0.015	4.84	17.89	2.51
Yamato-74646	1.96	1.01	0.03	4.59	19.02	1.94
(C-chondrite)						
Yamato-693 (c)	0.06	—	0.08	3.62	27.95	
Yamato-74662	—	—	0.06	7.38	22.53	
Makoia	0.00	0.00	0.00	6.74	25.43	
(Achondrite)						
Yamato-692 (b)	0.66	0.004	0.003	1.34	12.58	
Yamato-7308 (l)	0.39	0.012	0.007	0.75	16.00	

* The metallic phases of this chondrite are strongly weathered and the metals are oxidized or hydro-oxidized.

of ferromagnetic metal phase may serve as a reasonable measure to classify chondritic meteorites on the basis of the oxidization (or reduction) degree of metal phase of various chondrite groups in the Urey-Craig-Mason diagram and in the Prior diagram. As far as the magnetization intensity is concerned, the ferrimagnetic magnetization of magnetites or substituted magnetites can hardly be distinguished from the ferromagnetic magnetization of metals. However, the characteristic Curie point of the former can be clearly distinguished from Curie point and/or the phase-transition temperatures of the latter.

As for an indicator of the ferromagnetic magnetization of chondrites, GUS'KOVA and POCHTAREV (1969) and GUS'KOVA (1972) adopted the magnetic susceptibility (χ_0). Since, however, the magnetic susceptibility is subjected not only to the intrinsic ferromagnetic properties but also to the internal structures as well as grain sizes and shapes of ferromagnetic grains, it seems that the saturation

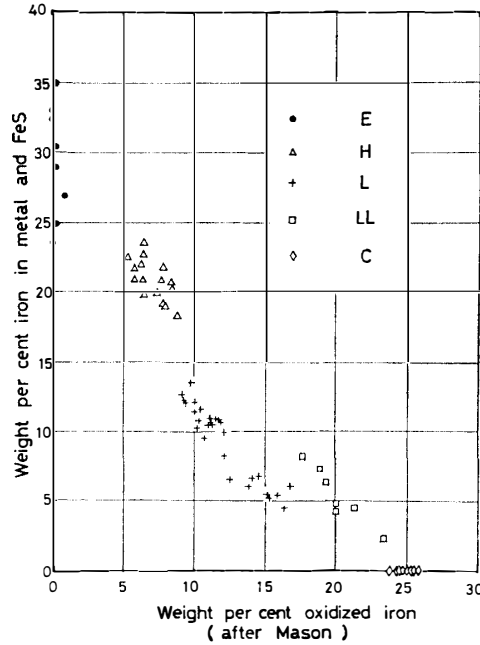


Fig. 1. Urey-Craig-Mason diagram to show a relationship between Fe in FeO and Fe in metal and FeS (after MASON, 1962).

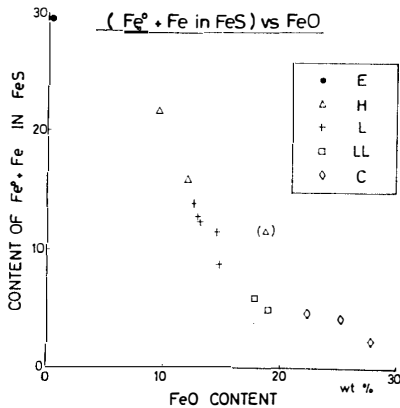


Fig. 2. Urey-Craig-Mason diagram for 14 recently analyzed chondrites.

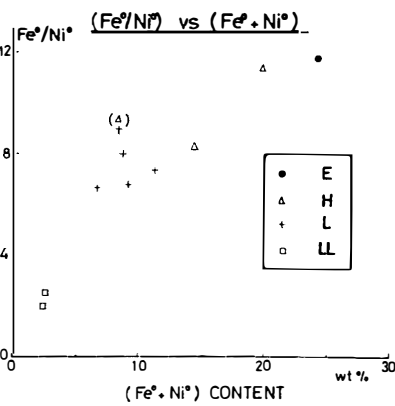


Fig. 3. Prior diagram to show a relationship between Fe^{2+}/Ni^{2+} and $Fe^{2+} + Ni^{2+}$ content for 11 recently analyzed chondrites (excluding 3 carbonaceous chondrites).

magnetization (I_s) which is dependent only on the composition and the content of ferromagnetic constituent is a better indicator of the ferromagnetic magnetization. NAGATA and SUGIURA (1976) therefore adopted I_s as the ferromagnetic magnetization indicator in their preliminary trial of a magnetic classification of stony

meteorites.

In the present study, which is a revision of the previous preliminary work by adding several new chemical and magnetic data of Antarctic stony meteorites including 2 LL-chondrites, the saturation magnetization, I_s , measured at various temperatures will be used for a possible magnetic classification of the stony meteorites.

2. Saturation Magnetization of Stony Chondrites at Room Temperature

The intensities of saturation magnetization (I_s) at room temperature of 13 chondrites and 2 achondrites measured by a vibration magnetometer in a magnetic field of 16 kOe are given in Table 2, and are plotted against the metallic phase contents represented by $(\text{Fe}^\circ + \text{Ni}^\circ)$ of individual samples in Fig. 4. An approximate linear relation between I_s and $(\text{Fe}^\circ + \text{Ni}^\circ)$, expressed by $I_s \simeq 200 (\text{Fe}^\circ + \text{Ni}^\circ)$ emu/gm, may be derived from Fig. 4. The derived coefficient, 200 emu/gm, ought to represent the average intensity of saturation magnetization of metallic grains contained in the stony meteorites. Since the specific intensity of saturation magnetization of pure iron at room temperature is 218 emu/gm, the average intensity of saturation magnetization of chondritic metals is a little smaller than that of pure iron. This result would indicate that the major component of metals in these meteorites is kamacite. However, the I_s -values of some individual stony meteorites are considerably smaller than those expected from their $(\text{Fe}^\circ + \text{Ni}^\circ)$ values. The observed defect of I_s of these chondrites is largely due to the coexistence of considerable portions of $\alpha + \gamma$ (plessite) and γ (taenite) phases together with α (kamacite) phase. Generally speaking, however, I_s -values of stony meteorites shown in Fig. 4 are reasonably well separately grouped for different types of stony meteorites, namely

$$I_s(E) > I_s(H) > I_s(L) > I_s(LL) > I_s(\text{achondrite}). \quad (1)$$

It seems likely, therefore, that the I_s -values can give rise to an approximate criterion for classifying the stony meteorites except for carbonaceous chondrites.

In Table 2, the observed values of I_s for one E-chondrite, 9 H-chondrites, 11 L-chondrites, 3 LL-chondrites, 6 C-chondrites and 3 achondrites are summarized. The distribution ranges of I_s -values are 24–40 emu/gm for H-chondrites, 7–23 emu/gm for L-chondrites, 3–6 emu/gm for LL-chondrites and < 1 emu/gm for achondrites. Although only one example of E-chondrite is available in the present study, a comparison of Fig. 2 and Fig. 4 with Fig. 1 may suggest $I_s > 40$ emu/gm for E-chondrites. Thus, we may provisionally suggest from these data,

$$I_s(E) > 40 \text{ emu/gm} > I_s(H) > 23 \text{ emu/gm} > I_s(L) > 6.5 \text{ emu/gm} \\ > I_s(LL) > 2 \text{ emu/gm} > I_s(\text{achondrite}). \quad (2)$$

This result may approximately correspond to the Urey-Craig-Mason law in regard

to the conservation of total Fe amount in chondritic meteorites. As the content of metallic iron is extremely small in achondrites in general (≤ 1.0 wt%) (e.g. MASON, 1962), their I_s -values also are distinctly small. The average I_s -values of H-, L-, LL-chondrites and achondrites are represented by $\bar{I}_s(\text{H})=(30.4\pm 4.7)$ emu/gm, $\bar{I}_s(\text{L})=(12.1\pm 3.4)$ emu/gm, $\bar{I}_s(\text{LL})=(4.7\pm 1.0)$ emu/gm and $\bar{I}_s(\text{achondrites})=(0.30\pm 0.16)$ emu/gm.

Table 2. Magnetic parameters of stony meteorites.

Meteorites	I_s (emu/gm)	θ_c^* (°C)	$\frac{I_s(\alpha)}{I_s}$	$\frac{I_s(\alpha+\gamma)}{I_s}$	$\frac{I_s(\gamma)}{I_s}$	$\left(\frac{I_s(\alpha_2)}{I_s}\right)$	$\left(\frac{I_s(\text{Mt})}{I_s}\right)$	Ni° Fe°+Ni° (wt%)
(E-chondrite) Yamato-691 (a)	48.0	764	97	0	3			5.6
(H-chondrite) Yamato-694 (d)	32.3	685	94	6	0			6.8
Yamato-7301 (j)*	(15.5)	660	(85)	10	5)			(10.9)
Yamato-74371	33.5	635	95	5	0			7.7
Yamato-74647	27.9	659	94	6	0			7.1
Kesen	34.4	670	95	5	0			6.5
Yonozu	24.2	654	87	13	0			10.2
Seminole	24.3	627	94	6	0			8.2
Mt. Baldr No. 2 (b)	27.4	650	88	10	2			9.5
Mt. Brown	40.0	640	90	5	5			9.9
(L-chondrite) Yamato-7305 (k)	14.3	624	38	0	0	(62)		10.3
Yamato-7304 (m)	16.6	644	90	0	10			10.2
Yamato-74191	6.8	671	79	21	0			11.6
Yamato-74362	8.1	645	81	19	0			11.4
Fukutomi	22.9	700	82	18	0			10.2
Mino	11.0	658	80	20	0			12.1
Allan Hills No. 9 (i)	8.4	680	65	35	0			15.7
Dalgety Down	9.7	648	85	14	0			10.5
Bjurböle	13.0	660	85	10	0			10.8
Barratta	12.0	655	80	15	3			11.6
Homestead	10.0	650	80	15	5			12.3
(LL-chondrite) Yamato-74442	6.0	680	45	35	20			22.6
Yamato-74646	3.2	720	19	7	74			31.0
St. Sererin	4.7	700	45	55	0			20.5
(C-chondrite) Yamato-693 (c)	10.8	540	0	0	0	(100)		
Yamato-74662	0.83	580	0	0	0	(100)		
Leoville	10.3	575	6	0	0	(94)		< 4
Allende	0.61	576	0	0	0	(100)		
Karoonda	7.8	548	0	0	0	(100)		
Makoia	8.0	570	0	0	0	(100)		
(Achondrite) Yamato-692 (b)	0.19	780	81	0	0	(19?)		< 4
Yamato-7308 (1)	0.53	792	100	0	0			< 4
Yamato-74013	0.17	792	56	0	0	(44?)		< 4

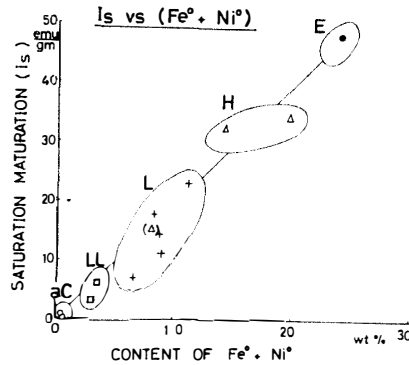


Fig. 4. Approximately linear relation between saturation magnetization (I_s) and $Fe^0 + Ni^0$ content for 13 recently analyzed stony meteorites (excluding 3 carbonaceous chondrites).

The main origin of magnetization of carbonaceous chondrites is the ferri-magnetic magnetites or substituted magnetites, and their I_s -values range from 0.6 to 11 emu/gm as given in Table 2. It seems likely that carbonaceous chondrites could be magnetically classified into two groups, *i.e.*, a group containing about 5–10 wt% of magnetite, I_s -value being 5–10 emu/gm, and another group containing less than 1 wt% of magnetite. According to LARSEN *et al.* (1974) and WATSON *et al.* (1975), the content of magnetite in C_1 and C_2 chondrites is less than 1 wt% in 11 specimens and ranges from 4 to 12 wt% in 7 specimens among 18 samples magnetically examined by them.

3. Thermomagnetic Characteristics of Stony Meteorites

As indicated by the Prior rule, the content of Ni^0 in metal phase in chondrites increases with a decrease of the $Fe^0 + Ni^0$ content and therefore E-, H-, L- and LL-chondrites are well separately grouped in their Fe^0/Ni^0 versus $Fe^0 + Ni^0$ diagram, as shown in Fig. 3. The Ni^0 content in metal phase in achondrites is, in general, extremely small. If the Ni^0 content in metal phase, represented by $Ni^0/(Fe^0 + Ni^0)$, is smaller than about 7 wt%, the metal phase forms a single α -phase, *i.e.*, kamacite. Kamacite is magnetically characterized by an irreversible but reproducible thermomagnetic curve, in which the $\alpha \rightarrow \gamma$ transition temperature ($\theta_{\alpha \rightarrow \gamma}^*$) in the heating curve is higher than the $\gamma \rightarrow \alpha$ transition temperature ($\theta_{\gamma \rightarrow \alpha}^*$) in the cooling curve. If, however, the Ni^0 content in α -phase is smaller than about 4 wt%, the thermomagnetic curve becomes apparently reversible, because Curie point of such a kamacite phase becomes smaller than its $\gamma \rightarrow \alpha$ transition temperature.

If the Ni^0 content exceeds 7 wt%, the metal phase splits into α -phase and $(\alpha + \gamma)$ -phase (plessite) or into α -phase and γ -phase (taenite). In practice, a perfect split into α - and γ -phases does not take place even in an extremely slowly cooled meteorite, but α -, $(\alpha + \gamma)$ - and γ -phases coexist in different ratios. Metals in most

H- and L-chondrites comprises α - and $(\alpha+\gamma)$ -phases as their major components, while those in some L-chondrites and LL-chondrites consist of α - and γ -phases with an additional portion of $(\alpha+\gamma)$ -phase.

Figs. 5, 6, 7 and 8 show respectively typical examples of thermomagnetic curves of an achondrite which contains Ni-poor α -phase metal, a H-chondrite which contains α -phase as the major component and $(\alpha+\gamma)$ -phase as a minor component, a L-chondrite which contains both α - and $(\alpha+\gamma)$ -phases, and a LL-chondrite which contains α -, $(\alpha+\gamma)$ - and γ -phases as the major components. The thermomagnetic curve of a Ni-poor α -phase is thermally reversible and has a magnetic transition temperature (Curie point) around 770°C. $\Theta_{\alpha\rightarrow\gamma}^*$ and $\Theta_{\gamma\rightarrow\alpha}^*$ -values of kamacite of 4–7 wt% Ni ranges from 768°C to 746°C and from 697°C to 600°C respectively. Since a difference of $\Theta_{\gamma\rightarrow\alpha}^*$ in the cooling process owing to a difference of Ni-content is much larger than that of $\Theta_{\alpha\rightarrow\gamma}^*$, the main magnetic transition temperature, *i.e.*, either Curie point or $\Theta_{\gamma\rightarrow\alpha}^*$, in the cooling process could be taken as an indicator of Ni-content for the kamacite phase of less than 7 wt% in Ni-content.

As shown in Figs. 6 and 7, an $(\alpha+\gamma)$ -phase disappears at the $\alpha\rightarrow\gamma$ transition temperature in the heating curve, being irreversibly transformed into a γ -phase, which is observable in the cooling curve, if the initial $(\alpha+\gamma)$ -phase is the fine-grained plessite. When $(\alpha+\gamma)$ -phase is the coarse-grained plessite, the $(\alpha+\gamma)$ -phase can not be completely transformed into a γ -phase by a single heat treatment, but can become a γ -phase by several repeated heat-treatments. The thermomagnetic curve after the transformation of $(\alpha+\gamma)$ -phase into a γ -phase comprises α -phase and γ -phase. The $(\alpha+\gamma)\rightarrow\gamma$ transition temperature, $\Theta_{(\alpha+\gamma)\rightarrow\gamma}^*$, in the first heating curve may represent the transformation of $(\alpha+\gamma)$ component of the minimum Ni-content to a γ -phase. The observed values of $\Theta_{(\alpha+\gamma)\rightarrow\gamma}^*$ range from about 540°C to 590°C, which suggests that the minimum Ni-content is 25–28 wt%. In other words, the $(\alpha+\gamma)$ -phase as a whole may include high-Ni components, in which the Ni-content is higher than the minimum Ni-content represented by $\Theta_{(\alpha+\gamma)\rightarrow\gamma}^*$.

As shown in Fig. 8, the magnetization of an LL-chondrite is largely due to the γ -phase magnetization together with smaller parts of the α - and the $(\alpha+\gamma)$ -magnetizations. An increase of Ni-content over 7 wt% in metal phase in chondrites thus results in a decrease of relative occupying ratio of α -phase and an increase of that of $(\alpha+\gamma)$ - and γ -phases. Hence, the percentage of α -phase magnetization in the total magnetization could be a criterion for classifying chondritic meteorites in accordance with the Prior rule.

Relative intensities of magnetizations of α -, $(\alpha+\gamma)$ - and γ -components of metal phases of all measured stony meteorites are summarized in Table 2, where (α_2) and (Mt) represent respectively α_2 -phase, which is caused by a remelting and subsequent rapid cooling, and magnetite phase. The relative occupation ratio of

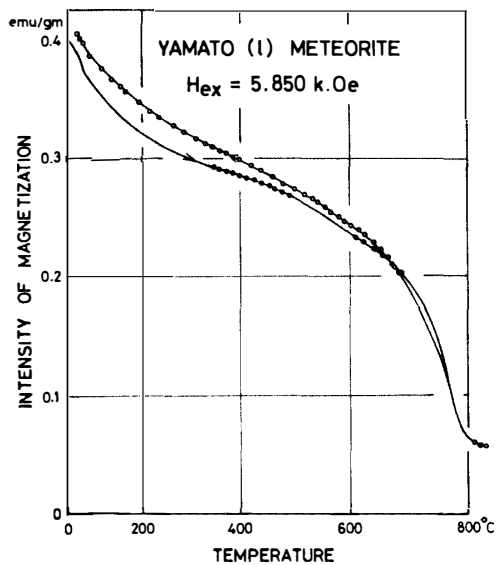


Fig. 5. Example of thermomagnetic curve of achondrite which contains Ni-poor kamacite only. (The magnetization in ordinates is the sum of ferromagnetization and paramagnetization of iron-oxide minerals.)

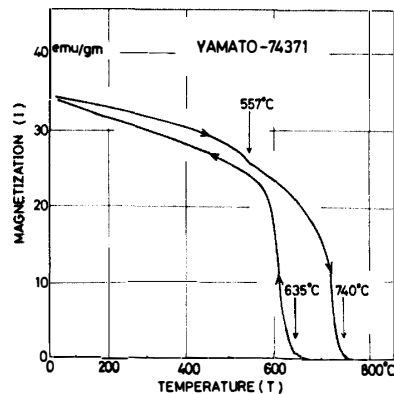


Fig. 6. Example of thermomagnetic curve of H-chondrite.

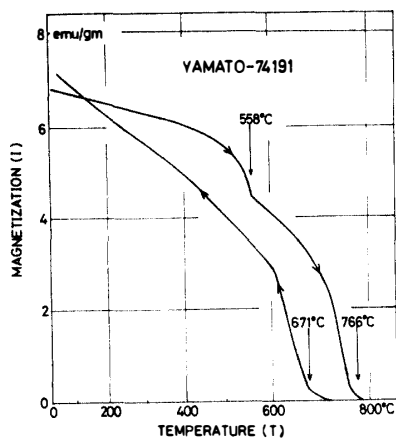


Fig. 7. Example of thermomagnetic curve of L-chondrite.

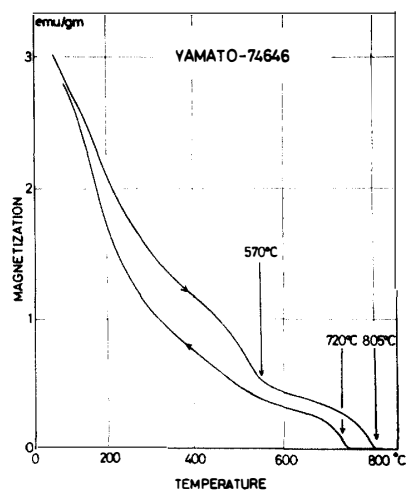


Fig. 8. Example of thermomagnetic curve of LL-chondrite.

α -phase is the largest in E-chondrites and decreases successively in H- and L-chondrites and finally in LL-chondrites.

In order to more quantitatively examine the relationship between the metallic phase composition and the Ni-content in the metal, approximate values of the Ni-content in metal phase will be estimated on the basis of thermomagnetic analysis of chondrites, the metallic compositions of which have been chemically analyzed. The Ni-content in α -phase can be estimated from the observed value of $\Theta_{\gamma \rightarrow \alpha}^*$, taking into consideration $\Theta_{\alpha \rightarrow \gamma}^* - \Theta_{\gamma \rightarrow \alpha}^* = \Delta\Theta^*$ also. The saturation magnetization of α -phase metal, $I_s(\alpha)$, may be approximately assumed to be about 210 emu/gm. The Ni-content and the saturation magnetization, $I_s(\gamma)$, of γ -phase may not be simple, because the Ni-content in meteoritic taenites has generally a continuous spectrum ranging from 25 to 50 wt%. However, results of magnetic analyses of γ -phase in chondritic metals (e.g. NAGATA, 1979) have suggested that the average values of Ni-content and saturation magnetization, can be approximately represented by 35 wt% and 120 emu/gm respectively. It is more difficult to estimate the average values of Ni-content and saturation magnetization, $I_s(\alpha + \gamma)$, for $(\alpha + \gamma)$ -phase. It has been suggested, however, that the average Ni-content of $(\alpha + \gamma)$ -phase is a little larger than its minimum Ni-content value (25–28 wt%) so that it could be assumed to be about 30 wt% (e.g. NAGATA, 1979). It is certain, on the other hand, that $I_s(\alpha + \gamma)$ is between $I_s(\alpha)$ and $I_s(\gamma)$, and $I_s(\alpha + \gamma)$ should depend on the relative amounts of α - and γ -phases. As the average Ni-content of $(\alpha + \gamma)$ -phase is assumed to be about 30 wt%, the $I_s(\alpha + \gamma)$ -value could be a little larger than the $I_s(\gamma)$ -value; namely $I_s(\alpha + \gamma) \simeq 150$ emu/gm is provisionally assumed in the present study.

On these assumptions, the average Ni-content in metal phase in chondrites can be evaluated. The average Ni-contents thus magnetically evaluated are compared with the corresponding chemical data in Table 3, where the Ni-contents in α -phase also are given for individual samples. As shown in Table 3 and in Fig. 9,

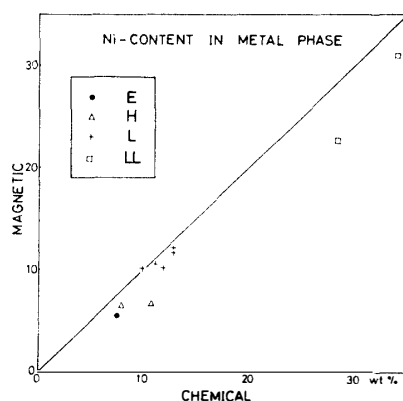


Fig. 9. Comparison of Ni-content in metal phase derived from magnetic data (in ordinates) with that chemically obtained (in abscissa) for 10 recently analyzed chondrites.

Table 3. Ni-content in metal phase in chondrites.

Chondrite	Ni-content (wt%)		
	α -phase	Bulk (magnetic)	Bulk (chemical)
(E-chondrite)			
Yamato-691 (a)	4.0	5.6	7.73
(H-chondrite)			
Yamato-694 (d)	4.3	6.8	10.83
Kesen	4.8	6.5	7.87
(L-chondrite)			
Yamato-7305 (k)	{ 6.0 (α) 13.0 (α_2) }	10.3	11.16
Yamato-7304 (m)	5.6	10.2	9.96
Yamato-74191	4.8	11.6	13.06
Fukutomi	4.3	10.2	11.92
Mino	5.7	12.1	12.86
(LL-chondrite)			
Yamato-74442	5.0	22.6	28.53
Yamato-74646	4.3	31.0	34.01

the Ni-contents magnetically evaluated are in approximate agreement with their chemically obtained values, though the former are a little smaller than the latter.

4. Magnetic Classifications of Stony Meteorites

As discussed in the preceding sections, I_s -values and thermomagnetic characteristics reasonably well represent the Urey-Craig-Mason law and the Prior rule respectively for classifying chondrites. The magnetic properties of achondrites seem to be represented by an extremely small value of I_s , which is mainly due to the metallic kamacite phase. On the basis of these magnetic properties, then, stony meteorites may be reasonably classified into various chemical groups.

4.1. I_s versus Ni-content in metal phase

As discussed in Section 3, the Ni-content in metal phase in stony meteorites can be approximately evaluated from the structure of their thermomagnetic curves which are generally composed of α -, ($\alpha+\gamma$)- and γ -phases of metallic FeNi alloy for E-, H-, L- and LL-chondrites and achondrites. The Ni-contents in metal phase thus magnetically evaluated are given in Table 2, and plotted against the I_s -values in Fig. 10. In this diagram, the chemical groups of chondrites, E, H, L and LL are well separately grouped. A H-chondrite within parentheses (Yamato-7301(j)) must be ignored because this chondrite is seriously weathered and oxidized (YAGI

et al., 1978). Fig. 10 is a kind of modified Prior diagram, since the Ni-content and I_s are represented by $\text{Ni}^\circ/(\text{Fe}^\circ + \text{Ni}^\circ)$ and $(\text{Fe}^\circ + \text{Ni}^\circ)$ respectively. In Fig. 10, carbonaceous chondrites are grouped within a domain of less than 12 emu/gm in I_s and less than 4% in the Ni-content. This grouping is due to their magnetic property that the ferromagnetic (ferrimagnetic) composition is only magnetite or substituted magnetite in most C-chondrites and some C-chondrites contain a small amount of kamacite, the Ni-content of which is less than 4%. The Ni-content in C-chondrites containing no metal is defined to be zero in this diagram. Thus, C-chondrites also are grouped well separated from the other chondrite groups in Fig. 10. Achondrites are characterized by their extremely small values of I_s and Ni-poor kamacite of their metal phase. In the diagram in Fig. 10, however, the domain of achondrite group is not clearly separated from the C-chondrite domain.

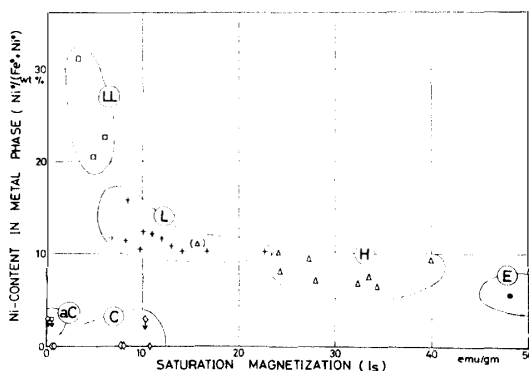


Fig. 10. $\text{Ni}^\circ/(\text{Fe}^\circ + \text{Ni}^\circ)$ versus I_s diagram to classify stony meteorites into 6 chemical groups.

4.2. I_s versus $I_s(\alpha)/I_s$

To clearly separate the achondrite group from the C-chondrite one, another two-dimensional diagram to represent the magnetic characteristics separately for all stony meteorite groups may be considered by use of the I_s -values and the ratio of magnetization of α -phase, $I_s(\alpha)$, to the total magnetization, I_s . The ratio $I_s(\alpha)/I_s$ is given for all measured samples in Table 2. In the I_s versus $I_s(\alpha)/I_s$ diagram shown in Fig. 11, all chemical groups of stony meteorites, *i.e.*, E-, H-, L-, LL- and C-chondrites and achondrites, are well grouped separately from one another. In Fig. 11, an H-chondrite in parentheses is a seriously weathered chondrite and the metal phase of an L-chondrite in parentheses comprises α - and α_2 -phases, suggesting remelting followed by rapid cooling of this chondrite. These two chondrites could therefore be eliminated from the diagram in Fig. 11.

An increase of $I_s(\alpha)/I_s$ with an increase of I_s from C-chondrites through LL-, L- and H-chondrites to E-chondrites indirectly represents an increase of $\text{Fe}^\circ/\text{Ni}^\circ$ with an increase of $\text{Fe}^\circ + \text{Ni}^\circ$, which is the Prior rule illustrated in Fig. 3. The achondrite group is characterized in Fig. 11 by a very small value of I_s and a

comparatively large value of $I_s(\alpha)/I_s$. Thus, the achondrite group is well separated from the C-chondrite group in the I_s versus $I_s(\alpha)/I_s$ diagram.

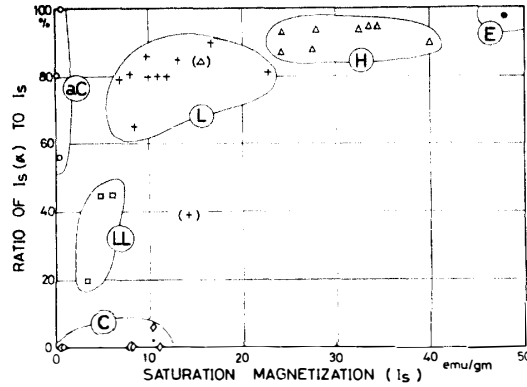


Fig. 11. $I_s(\alpha)/I_s$ versus I_s diagram to classify stony meteorites into 6 chemical groups.

4.3. I_s versus Θ_c^*

In a previous paper (NAGATA and SUGIURA, 1976), an expression of a magnetic classification of stony meteorites on a two-dimensional diagram of I_s versus the main magnetic transition temperature (Θ_c^*) in the cooling thermomagnetic curve has been proposed. Θ_c^* for this diagram is defined as either Curie point or the $\gamma \rightarrow \alpha$ transition temperature of α -phase, both of which can be clearly defined in the cooling thermomagnetic curve. The observed values of Θ_c^* are summarized also in Table 2. Θ_c^* values of H-, L- and LL-chondrites are always $\Theta_{\gamma \rightarrow \alpha}^*$ of their α -phase, ranging from 620°C to 720°C, whereas those of C-chondrites are always Curie points of magnetites or substituted magnetites, ranging from 540°C to 580°C. Since further α -phase in metal in E-chondrites and achondrites is generally nickel poor, their Θ_c^* values represent Curie points of the α -phase metal, ranging from 760°C to 790°C. Hence, Θ_c^* values of stony meteorites are classified

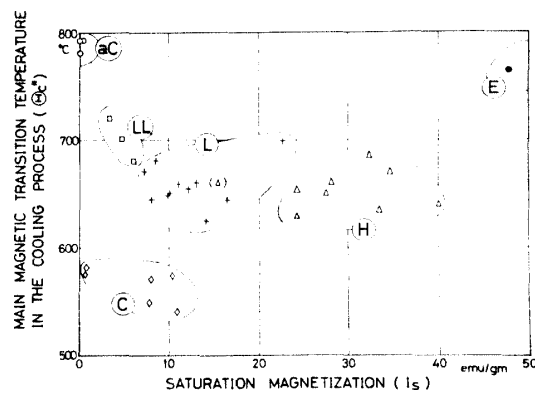


Fig. 12. Θ_c^* versus I_s diagram to classify stony meteorites into 6 chemical group.

into three groups, 760°–790°C for E-chondrites and achondrites, 620°–720°C for H-, L- and LL-chondrites, and 540°–580°C for C-chondrites. In Fig. 12, Θ_c^* values are plotted against I_s -values for all measured stony meteorites. In this diagram also, six chemical groups of stony meteorites are well grouped separately from one another.

5. Concluding Remarks

Summarizing the I_s versus ($\text{Ni}^0/(\text{Fe}^0 + \text{Ni}^0)$), I_s versus ($I_s(\alpha)/I_s$) and I_s versus Θ_c^* diagrams, we may obtain an overall view of the magnetic classification of stony meteorites as listed in Table 4. If the I_s -value only is taken into account, there

Table 4. Magnetic classifications of stony meteorites.

Meteorites	I_s (emu/gm)	$\frac{\text{Ni}^0}{\text{Fe}^0 + \text{Ni}^0}$ (wt %)	$I_s(\alpha)/I_s$ (%)	Θ_c^* (°C)
E-chondrite	40 <	< 6	95 <	~ 770
H-chondrite	23 ~ 40	7 ~ 10	87 ~ 95	630 ~ 690
L-chondrite	7 ~ 22	10 ~ 16	65 ~ 90	620 ~ 680
LL-chondrite	3 ~ 7	20 ~ 35	20 ~ 45	680 ~ 720
C-chondrite	0.5 ~ 11	≤ 3	0 ~ 6	540 ~ 580
Achondrite	0.2 ~ 0.5	≤ 3	55 ~ 100	~ 770

are a little overlap of the magnetite-rich C-chondrite group with the L- and LL-chondrite groups and that of the magnetite-poor C-chondrite group with the achondrite group. If the ratio $\text{Ni}^0/(\text{Fe}^0 + \text{Ni}^0)$ only is taken into consideration, there are partial overlaps among E-chondrites, C-chondrites and achondrites. There is an overlap of $I_s(\alpha)/I_s$ value among E-, H- and L-chondrites and achondrites. However, the $I_s(\alpha)/I_s$ value can be a definite measure scale to distinguish C-chondrites from the others. The Θ_c^* values also show overlaps between E-chondrites and achondrites and among H-, L- and LL-chondrites, but the Θ_c^* values of C-chondrites is uniquely separated. If, however, all four parameters given in Table 4 are simultaneously taken into account, the six stony meteorite groups could be almost definitely identified.

References

- GUS'KOVA, YE. G. (1972): The Magnetic Properties of Meteorites. Leningrad, Nauka Press, 143 p. (English translation, NASA TT F792, 1976).
 GUS'KOVA, E. G. and POCHTAREV, V. I. (1969): Magnetic properties of meteorites in the Soviet collection. Meteorite Research, ed. by P. M. Millman. Dordrecht, D. Reidel, 633–637.
 LARSEN, E. E., WATSON, D. E., HERNDON, J. M. and ROWE, M. W. (1974): Thermomagnetic

- analysis of meteorites 1 C₁ chondrites. *Earth Planet. Sci. Lett.*, **21**, 345–350.
- MASON, B. (1962): The classification of the chondritic meteorites. *Am. Mus. Novitates*, **2085**, 20 p.
- NAGATA, T. (1979): Magnetic properties of Yamato-7301(j), -7305(k) and -7304(m) chondrites in comparison with their mineralogical and chemical compositions. *Mem. Natl Inst. Polar Res., Spec. Issue*, **12**, 250–269.
- NAGATA, T. and SUGIURA, N. (1976): Magnetic characteristics of some Yamato meteorites—Magnetic classification of stone meteorites. *Mem. Natl Inst. Polar Res., Ser. C*, **10**, 30–58.
- PRIOR, G. T. (1920): The classification of meteorites. *Mineral. Mag.*, **19**, 51–63.
- UREY, H. C. and CRAIG, H. (1953): The composition of the stone meteorites and the origin of meteorites. *Geochim. Cosmochim. Acta.*, **4**, 36–82.
- WASILEWSKI, P. J. (1975): Magnetism of meteorites. Proceedings of Nagata Conference, ed. by R. M. FISHER *et al.* Greenbelt, Goddard Space Flight Center, 478–555.
- WATSON, D. E., LARSEN, E. E., HERNDON, J. M. and ROWE, M. W. (1975): Thermomagnetic analysis of meteorites 2. C₂ chondrites. *Earth Planet. Sci. Lett.*, **27**, 101–107.
- YAGI, K., LOVERING, J. F., SHIMA, M. and OKADA, A. (1978): Mineralogical and petrographical studies of the Yamato meteorites, Yamato-7301(j), -7305(k), -7308(l) and -7303(m) from Antarctica. *Mem. Natl Inst. Polar Res., Spec. Issue*, **8**, 121–141.

(Received May 17, 1978)